

New Edge-Directed Interpolation

Xin Li, *Member, IEEE*, and Michael T. Orchard, *Fellow, IEEE*

Abstract—This paper proposes an edge-directed interpolation algorithm for natural images. The basic idea is to first estimate local covariance coefficients from a low-resolution image and then use these covariance estimates to adapt the interpolation at a higher resolution based on the geometric duality between the low-resolution covariance and the high-resolution covariance. The edge-directed property of covariance-based adaptation attributes to its capability of tuning the interpolation coefficients to match an arbitrarily oriented step edge. A hybrid approach of switching between bilinear interpolation and covariance-based adaptive interpolation is proposed to reduce the overall computational complexity. Two important applications of the new interpolation algorithm are studied: resolution enhancement of grayscale images and reconstruction of color images from CCD samples. Simulation results demonstrate that our new interpolation algorithm substantially improves the subjective quality of the interpolated images over conventional linear interpolation.

Index Terms—Covariance-based adaptation, demosaicking, geometric regularity, image interpolation.

I. INTRODUCTION

IMAGE interpolation addresses the problem of generating a high-resolution image from its low-resolution version. The model employed to describe the relationship between high-resolution pixels and low-resolution pixels plays the critical role in the performance of an interpolation algorithm. Conventional linear interpolation schemes (e.g., bilinear and bicubic) based on space-invariant models fail to capture the fast evolving statistics around edges and consequently produce interpolated images with blurred edges and annoying artifacts. Linear interpolation is generally preferred not for the performance but for computational simplicity.

Many algorithms [1]–[12] have been proposed to improve the subjective quality of the interpolated images by imposing more accurate models. Adaptive interpolation techniques [1]–[4] spatially adapt the interpolation coefficients to better match the local structures around the edges. Iterative methods such as PDE-based schemes [5], [6] and projection onto convex sets (POCS) schemes [7], [8], constrain the edge continuity and find the appropriate solution through iterations. Edge-directed interpolation techniques [9], [10] employ a source model that emphasizes the visual integrity of the detected edges and modify the interpolation to fit the source model. Other approaches [11], [12] borrow the techniques from vector quantization (VQ) and morphological filtering to facilitate the induction of high-resolution images.

Manuscript received February 29, 2000; revised June 21, 2001. The associate editor coordinating the review of this manuscript and approving it for publication was Prof. Brian L. Evans.

X. Li is with Sharp Laboratories of America, Camas WA 98607 (e-mail: xli@sharplabs.com).

M. T. Orchard is with the Department of Electrical Engineering, Princeton University, Princeton NJ 08544 (email: orchard@ee.princeton.edu).

Publisher Item Identifier S 1057-7149(01)08203-3.

In this paper, we propose a novel noniterative orientation-adaptive interpolation scheme for natural-image sources. Our motivation comes from the fundamental property of an ideal step edge (known as geometric regularity [13]), i.e., that the image intensity field evolves more slowly *along* the edge orientation than *across* the edge orientation. Geometric regularity has important effects on the visual quality of a natural image such as the sharpness of edges and the freedom from artifacts. Since edges are presumably very important features in natural images, exploiting the geometric regularity of edges becomes paramount in many image processing tasks. In the scenario of image interpolation, an orientation-adaptive interpolation scheme exploits this geometric regularity.

Previous approaches to orientation adaptation [1], [3], [9] have proposed to explicitly estimate the edge orientation and accordingly tune the interpolation coefficients. However, these explicit approaches quantize the edge orientation into a finite number of choices (e.g., horizontal, vertical or diagonal) which affects the accuracy of the imposed edge model. In our previous work on edge-directed prediction for lossless image coding [14], we have shown that covariance-based adaptation is able to tune the prediction support to match an arbitrarily oriented edge. In this work, we extend the covariance-based adaptation method into a multiresolution framework. Though the covariance-based adaptation method dates back to two-dimensional (2-D) Kalman filtering [15], its multiresolution extension has not been addressed in the open literature.

The principal challenge of developing a multiresolution covariance-based adaptation method is how to obtain the high-resolution covariance from the available low-resolution image. The key in overcoming the above difficulty is to recognize the geometric duality between the low-resolution covariance and the high-resolution covariance which couple the pair of pixels along the same *orientation*. This duality enables us to estimate the high-resolution covariance from its low-resolution counterpart with a qualitative model characterizing the relationship between the covariance and the resolution, as we shall describe in Section II. With the estimated high-resolution covariance, the optimal minimum mean squared error (MMSE) interpolation can be easily derived by modeling the image as a locally stationary Gaussian process. Due to the effectiveness of covariance-based adaptive models, the derived interpolation scheme is truly orientation-adaptive and thus dramatically improves the subjective quality of the interpolated images over linear interpolation.

In spite of the impressive performance, the increased computational complexity of covariance-based adaptation is prohibitive. As shown in Section II, the complexity of covariance-based adaptive interpolation is about two orders of magnitude higher than that of linear interpolation. With the recognition of the fact that covariance-based adaptive

interpolation primarily improves the visual quality of the pixels around edges, we propose a hybrid approach to achieve a better tradeoff between visual quality and computational complexity. Covariance-based adaptive interpolation is only employed for the pixels around edges (“edge pixels”). For the pixels in the smooth regions (“nonedge pixels”), we still use bilinear interpolation due to its simplicity. Since edge pixels often consist of only a small fraction of pixels in the image, the hybrid approach effectively alleviates the burden of the computational complexity without sacrificing the performance.

We have studied two important applications related to image interpolation: resolution enhancement of a grayscale image [16] and reconstruction of a full-resolution color image from CCD samples (so-called “demaosaicking” problem [17]). Our new edge-directed interpolation algorithm can be easily applied in both applications. In particular, for the demosaicking problem, we also consider the interpolation in the color-difference space in order to exploit the dependency among the color planes as suggested by [18], [19]. We use extensive simulation results to demonstrate that new edge-directed interpolation significantly improves the visual quality of the reconstructed images over linear interpolation in both applications.

It is generally agreed that peak signal-to-noise ratio (PSNR) does not always provide an accurate measure of the visual quality for natural images except in the case that the only source of degradation is additive white noise. Though there exist other objective image quality metrics such as degradation-based quality measures [20], we find that the artifacts related to the orientation of edges (e.g., jaggy artifacts) are not predicted by the degradation models considered in [20]. Though it is possible to apply the fan filters to decompose an image into different orientation bands and take the masking effect into account by distinguishing in-band and out-of-band noise [21], the overall vision model becomes too complicated and is out of the scope of this paper. Therefore, we shall only rely on subjective evaluation to assess the visual quality of the interpolated images in this paper. Fortunately, the improvements brought by new edge-directed interpolation over linear interpolation can often be easily observed when the interpolated images are viewed at a normal distance.

The rest of this paper is organized as follows. Section II presents the new edge-directed interpolation algorithm. Section III studies two applications of the proposed interpolation scheme. Simulation results are reported in Section IV and some concluding remarks are made in Section V.

II. NEW EDGE-DIRECTED INTERPOLATION

Without the loss of generality, we assume that the low-resolution image $X_{i,j}$ of size $H \times W$ directly comes from of size of $2H \times 2W$, i.e., $Y_{2i,2j} = X_{i,j}$. We use the following basic problem to introduce our new interpolation algorithm: How do we interpolate the interlacing lattice $Y_{2i+1,2j+1}$ from the lattice $Y_{2i,2j} = X_{i,j}$. We constrain ourselves to the fourth-order linear interpolation (refer to Fig. 1)

$$\hat{Y}_{2i+1,2j+1} = \sum_{k=0}^1 \sum_{l=0}^1 \alpha_{2k+l} Y_{2(i+k),2(j+l)} \quad (1)$$

where the interpolation includes the four nearest neighbors along the diagonal directions.

A reasonable assumption made with the natural image source is that it can be modeled as a locally stationary Gaussian process. According to classical Wiener filtering theory [22], the optimal MMSE linear interpolation coefficients are given by

$$\vec{\alpha} = R^{-1} \vec{r} \quad (2)$$

where $R = [R_{kl}]$, ($0 \leq k, l \leq 3$) and $\vec{r} = [r_k]$, ($0 \leq k \leq 3$) are the local covariances at the high resolution (we call them “high-resolution covariances” throughout this paper). For example, r_0 is defined by $E[Y_{2i,2j} Y_{2i+1,2j+1}]$, as shown in Fig. 1. A practical approach to obtain the expectation is to average over a collection of the observation data. However, since $Y_{2i+1,2j+1}$ is the missing pixel we want to interpolate, the following question emerges naturally: is it possible to obtain the knowledge of high-resolution covariances when we have access to only the low-resolution image?

The answer is affirmative for the class of ideal step edges that have an infinite scale (the case of other edge models with a finite scale will be discussed later). We propose to estimate the high-resolution covariance from its low-resolution counterpart with a qualitative model characterizing the relationship between the *covariance* and the *resolution*. Let us start from an ideal step edge model in the one-dimensional (1-D) case. We denote the sampling distance at the low and the high resolution by $2d$ and d respectively. Under the locally stationary Gaussian assumption, the relationship between the normalized covariance and the sampling distance x can be approximated by a function $R(x) \sim e^{-x^2/2\sigma^2}$. It follows that the high-resolution covariance is linked to the low-resolution covariance by a quadratic-root function $R(d) = R(2d)^{1/4}$. Asymptotically as the sampling distance d goes to 0, $R(d)$ can be approximately replaced by $R(2d)$ for the simplicity of computation.

For 2-D signals such as images, *orientation* is another important factor for successfully acquiring the knowledge of high-resolution covariances. One of the fundamental property of edges is the so-called “geometric regularity” [13]. Geometric regularity of edges refers to the sharpness constraint *across* the edge orientation and the smoothness constraint *along* the edge orientation. Such orientation-related property of edges directly affects the visual quality around edge areas. It should be noted that the local covariance structure contains sufficient information to determine the orientation. However, we do not want to estimate the orientation from the local covariances due to the limitations of the explicit approaches described before. Instead, we propose to estimate the high-resolution covariance from its low-resolution counterpart based on their intrinsic “geometric duality.”

Geometric duality refers to the correspondence between the high-resolution covariance and the low-resolution covariance that couple the pair of pixels at the different resolution but along the same orientation. Fig. 1 shows the geometric duality between the high-resolution covariance R_{kl}, r_k and the low-resolution covariance \hat{R}_{kl}, \hat{r}_k when we interpolate the interlacing lattice $Y_{2i+1,2j+1}$ from $Y_{2i,2j}$. Geometric duality facilitates the estimation of local covariance for 2-D signals without the necessity of explicitly estimating the edge orientation. Similar geo-

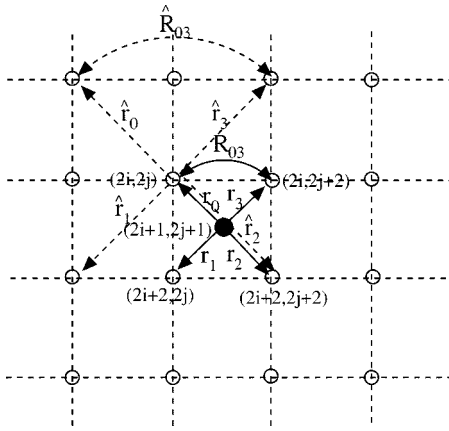


Fig. 1. Geometric duality when interpolating $Y_{2i+1,2j+1}$ from $Y_{2i,2j}$.

metric duality can also be observed in Fig. 2 when interpolating the interlacing lattice $Y_{i,j}(i+j = \text{odd})$ from the lattice $Y_{i,j}(i+j = \text{even})$. In fact, Figs. 1 and 2 are isomorphic up to a scaling factor of $2^{1/2}$ and a rotation factor of $\pi/4$.

As long as the correspondence between the high-resolution covariance and the low-resolution covariance is established, it becomes straightforward to link the existing covariance estimation method and covariance-based adaptation method together. The low-resolution covariance \hat{R}_{kl}, \hat{r}_k can be easily estimated from a local window of the low-resolution image using the classical covariance method [22]

$$\hat{R} = \frac{1}{M^2} C^T C, \hat{r} = \frac{1}{M^2} C^T \vec{y} \quad (3)$$

where $\vec{y} = [y_1 \dots y_k \dots y_{M^2}]^T$ is the data vector containing the $M \times M$ pixels inside the local window and C is a $4 \times M^2$ data matrix whose k th column vector is the four nearest neighbors of y_k along the diagonal direction. According to (2) and (3), we have

$$\vec{\alpha} = (C^T C)^{-1} (C^T \vec{y}). \quad (4)$$

Therefore, the interpolated value of $Y_{2i+1,2j+1}$ can be obtained by substituting (4) into (1).

The edge-directed property of covariance-based adaptation comes from its ability to tune the interpolation coefficients to match an arbitrarily-oriented step edge. Detailed justification of such orientation-adaptive property can be found in [14]. However, for the class of edge models with finite scales (e.g., tightly packed edges that can be commonly found in the texture patterns), frequency aliasing due to the downsampling operation can affect the preservation of the true edge orientation. When the scale of edges introduced by the distance between adjacent edges becomes comparable to the sampling distance d , the aliasing components significantly overlap with the original components and might introduce phantom dominant linear features in the frequency domain. Such phenomena will not affect the visual quality of the interpolated image but will affect its fidelity to the original image.

The principal drawback with covariance-based adaptive interpolation is its prohibitive computational complexity. For example, when the size of the local window is chosen to be $M = 8$,

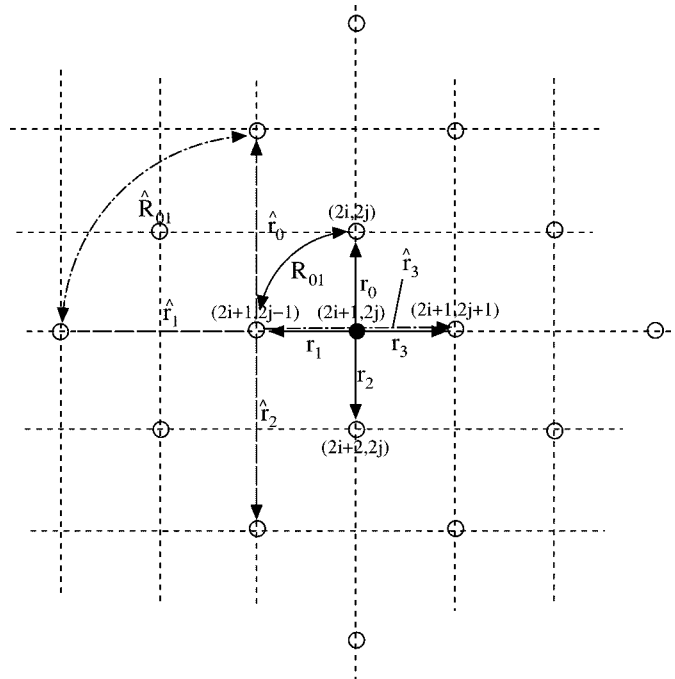


Fig. 2. Geometric duality when interpolating $Y_{i,j}(i+j = \text{odd})$ from $Y_{i,j}(i+j = \text{even})$.

the computation of (4) requires about 1300 multiplications per pixel. If we apply covariance-based adaptive interpolation to all the pixels, then the overall complexity would be increased by about two orders of magnitude when compared to that of linear interpolation. In order to manage the computational complexity, we propose the following hybrid approach: covariance-based adaptive interpolation is only applied to edge pixels (pixels near an edge); for nonedge pixels (pixels in smooth regions), we still use simple bilinear interpolation. Such a hybrid approach is based on the observation that only edge pixels benefit from the covariance-based adaptation and edge pixels often consist of a small fraction of the whole image. A pixel is declared to be an edge pixel if an activity measure (e.g., the local variance estimated from the nearest four neighbors) is above a preselected threshold Th . Since the computation of the activity measure is typically negligible when compared to that of covariance estimation, dramatic reduction of complexity can be achieved for images containing a small fraction of edge pixels. We have found that the percentage of edge pixels ranges from 5% to 15% for the test images used in our experiments, which implies a speed-up factor of 7–20.

III. APPLICATIONS

A. Resolution Enhancement of Grayscale Images

The new edge-directed interpolation algorithm can be used to magnify the size of a grayscale image by any factor that is a power of two along each dimension. In the basic case where the magnification factor is just two, the resizing scheme consists of two steps: the first step is to interpolate the interlacing lattice $Y_{2i+1,2j+1}$ from the lattice $Y_{2i,2j}$; and the second step is to interpolate the other interlacing lattice $Y_{i,j}(i+j = \text{odd})$ from the lattice $Y_{i,j}(i+j = \text{even})$. The algorithm described in

Section II can be directly applied to the first step. As we mentioned earlier, the second step (Fig. 2), if rotated by 45° along the counter-clockwise direction and scaled by a factor of $2^{1/2}$, becomes exactly the same as the first step (Fig. 1). Therefore, the implementation of the second step is almost identical to that of the first step except the labeling of the data matrix C and the data vector \vec{y} .

B. Demosaicking of Color CCD Samples

Another important industrial application of new edge-directed interpolation is the so-called “demosaicking” problem [17], i.e., the reconstruction of a full-resolution color image from CCD samples generated by the Bayer color filter array (CFA), as shown in Fig. 3. It is easy to see that our algorithm easily lends itself to the demosaicking problem. Two-step algorithm described in Section III-A can be directly used to interpolate the missing red and blue pixels; and only the second step is needed for the green pixels. However, the approaches of treating (R,G,B) planes independently ignore the strong dependency among the color planes and annoying artifacts brought by the color misregistration are often visible in the reconstructed color images.

Recent demosaicking methods [17]–[19] have shown that the performance of CFA interpolation can be significantly improved by exploiting the interplane dependency. In particular, [18] and [19] advocate the interpolation in the color-difference space instead of the original color space. More specifically, they consider the color difference $K_R = R - G$ and $K_B = B - G$ during the interpolation. For example, when interpolating the missing green pixel at the location of a Red pixel (refer to Fig. 3), instead of recovering it by the average of the four surrounding green pixels, the color difference K_R is interpolated from the average of the four surrounding K_R values at the green pixels and then the Green pixel is recovered by $G = R - K_R$. The missing green pixels at the locations of the blue pixels can also be recovered in a similar fashion and the interpolation of the missing red and blue pixels follows the same philosophy.

The underlying assumption made by the interpolation in the color-difference space is that the color difference is locally constant. Though such an assumption is valid within the boundary of an object, it often gets violated around edges in color images. If linear interpolation is employed, the problem of color misregistration still exists around edges where the color difference experiences a sharp transition. Our new edge-directed interpolation effectively solves this problem by interpolating along the edge orientation in the color-difference space. By avoiding the interpolation across the edge orientation in the color-difference space, we successfully get rid of the artifacts brought by the color misregistration and further improve the subjective quality of the reconstructed image. Such improvement can be clearly seen from the simulation results reported in the next section.

IV. SIMULATION RESULTS

As mentioned in the introduction, most existing objective metrics of image quality cannot take the visual masking effect around an arbitrarily-oriented edge into account. Therefore,

G	R	G	R	G	R
B	G	B	G	B	G
G	R	G	R	G	R
B	G	B	G	B	G
G	R	G	R	G	R
B	G	B	G	B	G

Fig. 3. Bayer color filter array pattern (U.S. Patent 3 971 065, issued 1976).

we shall only rely on subjective evaluation to assess the visual quality of the interpolated images. We believe that the improvements on visual quality brought by new edge-directed interpolation can be easily observed when the images are viewed at a normal distance.

We have used four photographic images: Airplane, Cap, Motor, and Parrot as our benchmark images. The original 24-bit color images are 768×512 (around 1 MB). Photographic images in this range (with the resolution of 0.25 M–1 M pixels) are widely available in current digital camera products. Two sets of experiments have been used to evaluate the effectiveness of the proposed interpolation algorithm: one for grayscale images and the other for color images.

In the first set of experiments with grayscale images, we use the luminance components of the four color images. The new edge-directed interpolation is compared with two conventional linear interpolation methods: bilinear and bicubic. The low-resolution image (with the size of 384×256) is obtained by direct downsampling the original image by a factor of two along each dimension (aliasing is introduced). The implementations of bilinear and bicubic interpolation are taken from MATLAB 5.1 [23]. In our implementation of new edge-directed interpolation algorithm, the window size M and the threshold to declare an edge pixel Th are both set to be 8. Figs. 4–7 include the comparison of the portions of the interpolated images. We can observe that annoying ringing artifacts are dramatically suppressed in the interpolated images by our scheme due to the orientation adaptation. In terms of complexity, the running time of linear interpolation is less than 1 s; while the proposed edge-directed interpolation requires 5–10 s, depending on the percentage of edge pixels in the image. Therefore, the overall complexity of our scheme even with the switching strategy is still over an order of magnitude higher than that of linear interpolation.

In the second set of experiments, we implement three demosaicking schemes for color images: scheme 1 is based on linear interpolation techniques in the original color space; scheme 2 uses linear interpolation techniques in the color-difference space as does [19]; and scheme 3 employs new edge-directed interpolation in the color-difference space. Figs. 8 and 9 shows the portions of the interpolated color Parrot image and their close-up comparisons. It can be observed that scheme 3 generates the image with the highest visual quality. Interpolation in the color-difference space suppresses the artifacts associated with color misregistration, as we compare Figs. 9(b) and (c). But Fig. 9(c) still suffers from noticeable dotted artifacts around the top of the parrot where there is a sharp color transition. New edge-directed interpolation better preserves the geometric regularity

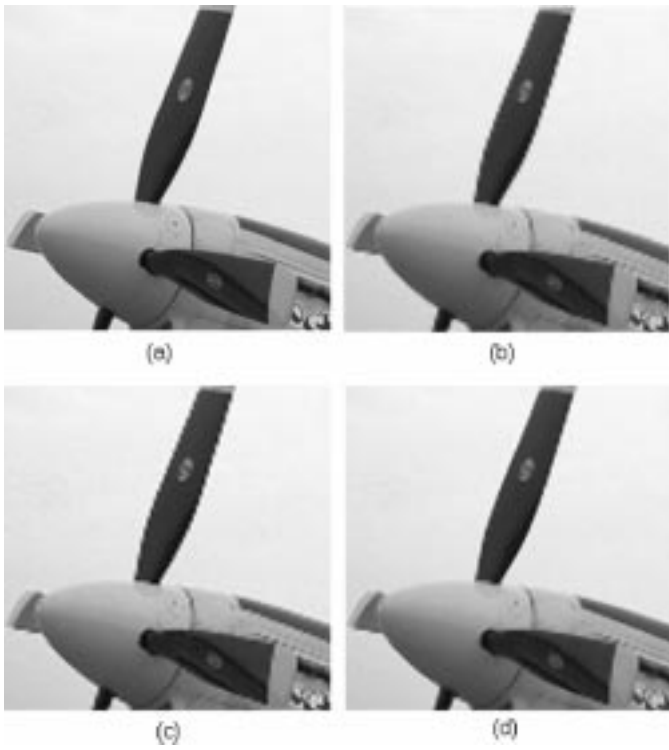


Fig. 4. Portions of (a) original Airplane image, (b) reconstructed image by bilinear interpolation, (c) reconstructed image by bicubic interpolation, and (d) reconstructed image by new edge-directed interpolation.

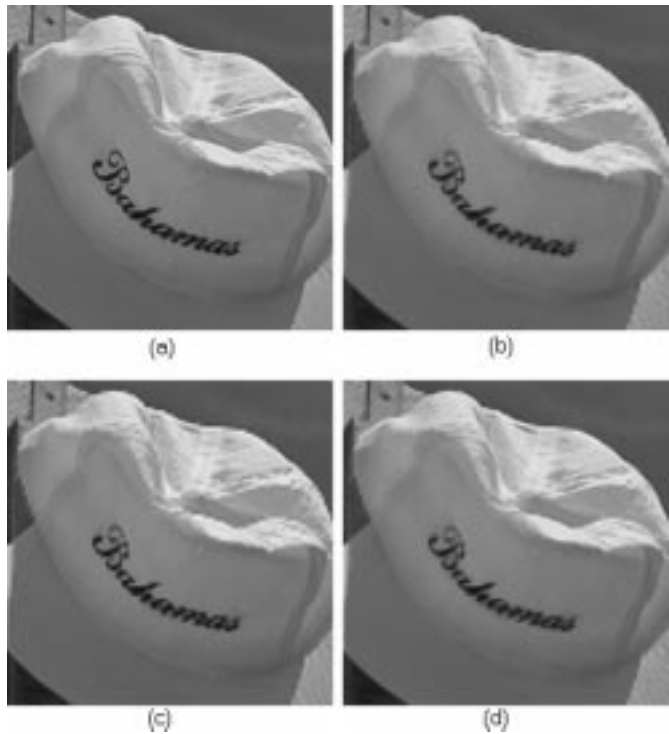


Fig. 5. Portions of (a) original Cap image, (b) reconstructed image by bilinear interpolation, (c) reconstructed image by bicubic interpolation, and (d) reconstructed image by new edge-directed interpolation.

around the color edges and thus generates interpolated images with higher visual quality.

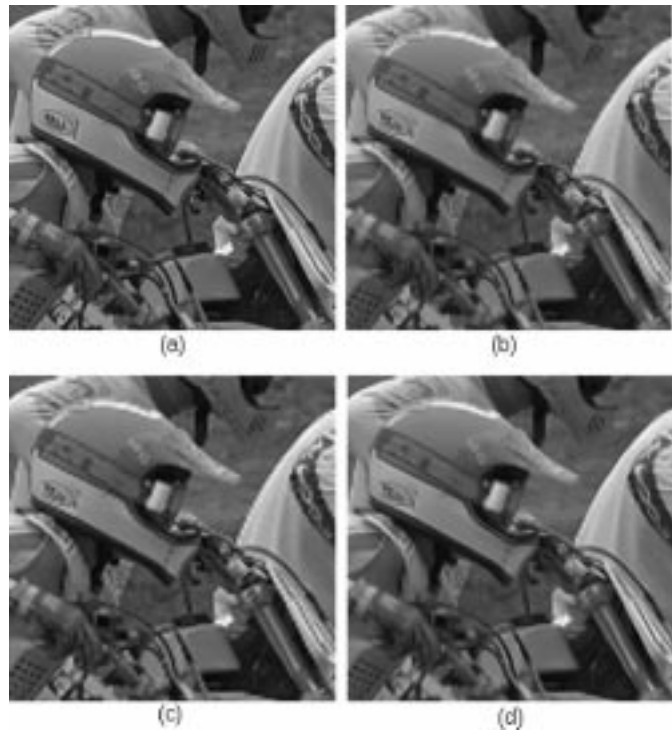


Fig. 6. Portions of (a) original Motor image, (b) reconstructed image by bilinear interpolation, (c) reconstructed image by bicubic interpolation, and (d) reconstructed image by new edge-directed interpolation.

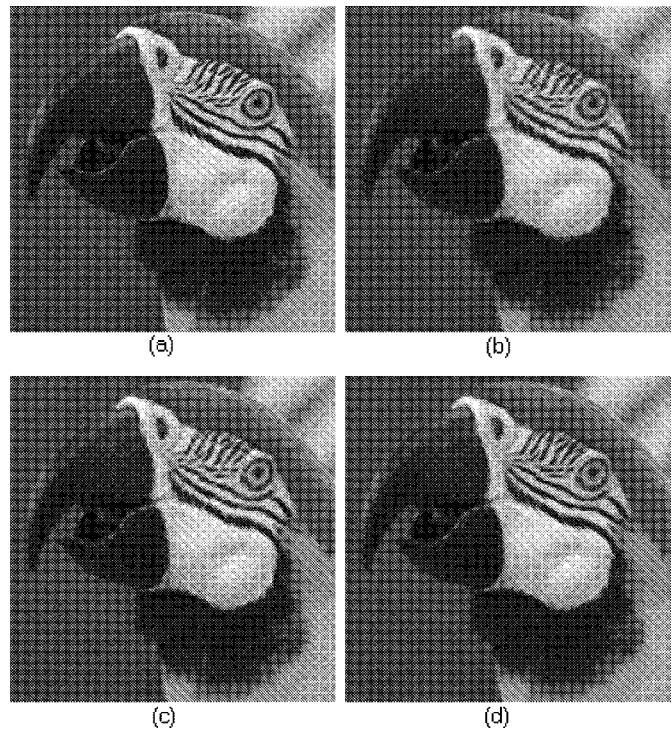


Fig. 7. Portions of (a) original Parrot image, (b) reconstructed image by bilinear interpolation in the, (c) reconstructed image by bicubic interpolation, and (d) reconstructed image by new edge-directed interpolation.

V. CONCLUDING REMARKS

In this paper, we present a novel edge-directed interpolation algorithm. The interpolation is adapted by the local covariance

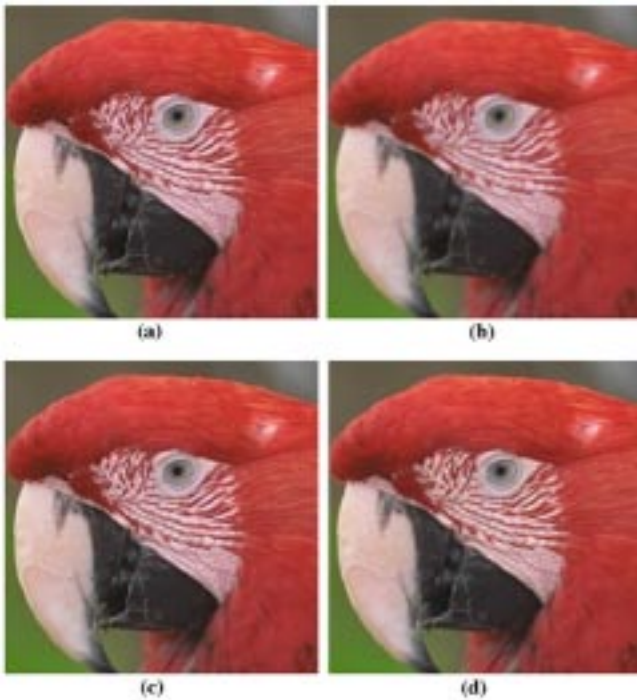


Fig. 8. Portions of (a) original Parrot image, (b) reconstructed image by bilinear interpolation in the original color space, (c) reconstructed image by bilinear interpolation in the color-difference space, and (d) reconstructed image by new edge-directed interpolation in the color-difference space.

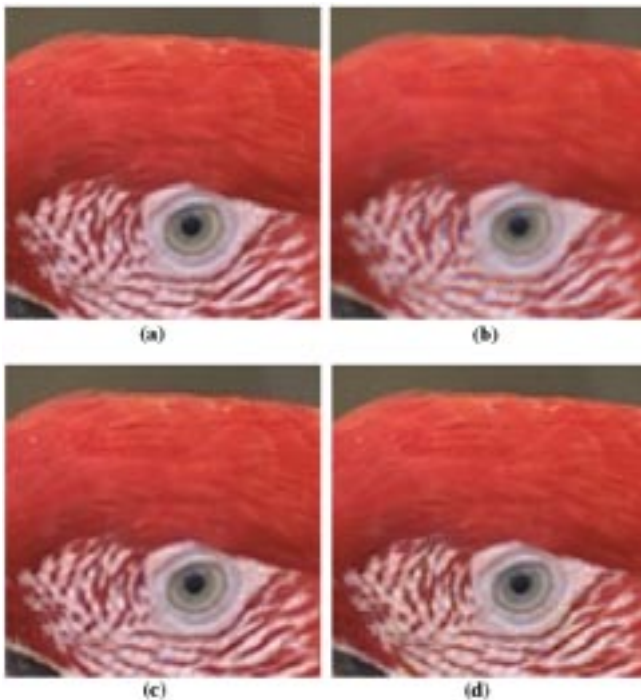


Fig. 9. Close-up comparison of (a) original Parrot image, (b) reconstructed image by bilinear interpolation in the original color space, (c) reconstructed image by bilinear interpolation in the color-difference space, and (d) reconstructed image by new edge-directed interpolation in the color-difference space.

and we provide a solution to estimate the high-resolution covariance from the low-resolution counterpart based on their geometric duality. A hybrid scheme of combining bilinear interpo-

lation and covariance-based adaptive interpolation is proposed to alleviate the burden of the computational complexity. We have studied two important applications of our new interpolation algorithm: resolution enhancement of grayscale images and demosaicking of color CCD samples. In both applications, new edge-directed interpolation demonstrates significant improvements over linear interpolation on visual quality of the interpolated images.

ACKNOWLEDGMENT

The authors thank the associate editor for his insightful suggestions and anonymous reviewers for their critical comments, which help to improve the presentation of this paper. The first author thanks I. K. Tam at National Taiwan University for providing the four test images and S. Daly at Sharp Labs of America for discussions on image quality assessment.

REFERENCES

- [1] V. R. Algazi, G. E. Ford, and R. Potharlanka, "Directional interpolation of images based on visual properties and rank order filtering," in *Proc. IEEE Int. Conf. Acoustics, Speech, Signal Processing*, vol. 4, 1991, pp. 3005–3008.
- [2] S. W. Lee and J. K. Paik, "Image interpolation using adaptive fast B-spline filtering," in *Proc. IEEE Int. Conf. Acoustics, Speech, Signal Processing*, vol. 5, 1993, pp. 177–180.
- [3] J. E. Adams Jr, "Interactions between color plane interpolation and other image processing functions in electronic photography," *Proc. SPIE*, vol. 2416, pp. 144–151, 1995.
- [4] S. Carrato, G. Ramponi, and S. Marsi, "A simple edge-sensitive image interpolation filter," in *Proc. IEEE Int. Conf. Image Processing*, vol. 3, 1996, pp. 711–714.
- [5] B. Ayazifar and J. S. Lim, "Pel-adaptive model-based interpolation of spatially subsampled images," in *Proc. IEEE Int. Conf. Acoustics, Speech, Signal Processing*, vol. 3, 1992, pp. 181–184.
- [6] B. S. Morse and D. Schwartzwald, "Isophote-based interpolation," in *Proc. IEEE Int. Conf. Image Processing*, vol. 3, 1998, pp. 227–231.
- [7] K. Ratakonda and N. Ahuja, "POCS based adaptive image magnification," in *Proc. IEEE Int. Conf. Image Processing*, vol. 3, 1998, pp. 203–207.
- [8] D. Calle and A. Montanvert, "Superresolution inducing of an image," in *Proc. IEEE Int. Conf. Image Processing*, vol. 3, 1998, pp. 232–235.
- [9] K. Jensen and D. Anastassiou, "Subpixel edge localization and the interpolation of still images," *IEEE Trans. on Image Processing*, vol. 4, pp. 285–295, Mar. 1995.
- [10] J. Allebach and P. W. Wong, "Edge-directed interpolation," in *Proc. IEEE Int. Conf. Image Processing*, vol. 3, 1996, pp. 707–710.
- [11] D. A. Florencio and R. W. Schafer, "Post-sampling aliasing control for natural images," in *Proc. IEEE Int. Conf. Acoustics, Speech, Signal Processing*, vol. 2, 1995, pp. 893–896.
- [12] F. Fekri, R. M. Mersereau, and R. W. Schafer, "A generalized interpolative VQ method for jointly optimal quantization and interpolation of images," in *Proc. IEEE Int. Conf. Acoustics, Speech, Signal Processing*, vol. 5, 1998, pp. 2657–2660.
- [13] S. G. Mallat, *A Wavelet Tour of Signal Processing*. New York: Academic, 1998.
- [14] X. Li and M. Orchard, "Edge directed prediction for lossless compression of natural images," *IEEE Trans. Image Processing*, vol. 10, pp. 813–817, June 2001.
- [15] J. W. Woods, "Two-dimensional Kalman filters," in *Two-Dimensional Digital Signal Processing*, T. S. Huang, Ed. New York: Springer-Verlag, 1981, vol. 42, pp. 155–205.
- [16] X. Li and M. Orchard, "New edge directed interpolation," in *Proc. IEEE Int. Conf. Image Processing*, vol. 2, 2000, pp. 311–314.
- [17] R. Kimmel, "Demosaicing: Image reconstruction from color CCD samples," *IEEE Trans. Image Processing*, vol. 8, pp. 1221–1228, Sept. 1999.
- [18] J. E. Adams Jr, "Design of practical color filter array interpolation algorithms for digital cameras," *Proc. SPIE*, vol. 3028, pp. 117–125, 1997.
- [19] S. C. Pei and I. K. Tam, "Effective color interpolation in CCD color filter array using signal correlation," in *Proc. IEEE Int. Conf. Image Processing*, vol. 3, 2000, pp. 488–491.

- [20] N. Damera-Venkata, T. D. Kite, W. S. Geisler, B. L. Evans, and A. C. Bovik, "Image quality assessment based on a degradation model," *IEEE Trans. Image Processing*, vol. 9, pp. 636–650, Apr. 2000.
- [21] S. Daly, "The visible differences predictor: An algorithm for the assessment of image fidelity," in *Digital Images and Human Vision*, A. Watson, Ed. Cambridge, MA: MIT Press, 1993.
- [22] N. Jayant and P. Noll, *Digital Coding of Waveforms: Principles and Applications to Speech and Video*. Englewood Cliffs, NJ: Prentice-Hall, 1984.
- [23] D. Hanselman and B. Littlefield, *Mastering MATLAB 5: A Comprehensive Tutorial and Reference*. Englewood Cliffs, NJ: Prentice-Hall, 1998.



Xin Li (S'97-M'00) received the B.S. degree with highest honors in electronic engineering and information science from University of Science and Technology of China, Hefei, in 1996 and the Ph.D. degree in electrical engineering from Princeton University, Princeton, NJ, in 2000.

He has been Member of Technical Staff with Sharp Laboratories of America, Camas, WA, since August 2000. His research interests include image/video coding and processing.

Dr. Li received the Best Student Paper Award at the Conference of Visual Communications and Image Processing, San Jose, CA, in January 2001.



Michael T. Orchard (F'00) was born in Shanghai, China. He received the B.S. and M.S. degrees in electrical engineering from San Diego State University, San Diego, CA, in 1980 and 1986, respectively and the M.A. and Ph.D. degrees in electrical engineering from Princeton University, Princeton, NJ, in 1988 and 1990, respectively.

He was with the Government Products Division, Scientific Atlanta, Atlanta, GA, from 1982 to 1986, developing passive sonar DSP applications and has consulted with the Visual Communication

Department of AT&T Bell Laboratories since 1988. From 1990 to 1995, he was an Assistant Professor with the Department of Electrical and Computer Engineering, University of Illinois at Urbana-Champaign, where he served as Associate Director of Image Laboratory, Beckman Institute. Since 1995, he has been an Associate Professor with the Department of Electrical Engineering, Princeton University. During the spring of 2000, he served as Texas Instruments Visiting Professor at Rice University, Houston, TX.

Dr. Orchard received the National Science Foundation Young Investigator Award in 1993, the Army Research Office Young Investigator Award in 1996, and was elected IEEE Fellow in 2000 for "contribution to the theory and development of image and video compression algorithms."